

POWERED AERO-GRAVITY ASSISTED MANEUVERS IN VENUS AND MARS CHANGING THE BANK ANGLE OF THE SPACECRAFT

Jhonathan O. Murcia P.,* and Antonio F.B.A. Prado †

In a three body system, with the Sun as the massive body, a planet as secondary body and a spacecraft as a massless body, the change in the spacecraft trajectory due to a close approach with the planet is known as a gravity-assisted maneuver. If the planet has atmosphere and the pericenter of the spacecraft is lower than the atmospheric limit, the aerodynamic forces affect the gravity-assist, and the new maneuver is known as aero-gravity assisted. Including an instantaneous impulse in the pericenter, it is created the powered aero-gravity-assisted maneuver. The present paper uses this type of maneuver considering Drag, Lift and the bank angle to control the Lift direction. With this maneuver, it is possible to make energy and inclination changes in the trajectory of the spacecraft, which are very expensive maneuvers. A value of $L/D = 9.0$ is used to represent the maximum value used by waveriders spacecrafts to get maximum effects of Lift. Due to the proximity with the Earth, the presence of planetary atmosphere and applications in previous gravity assisted maneuvers, the planets Venus and Mars are selected to be used in the numerical simulations. A RKF 7/8 integrator with adaptive step is implemented. To observe the influence of Lift and Drag, the ballistics coefficient changes from 0.0 to 5×10^{-7} km^2/kg and the impulse at the pericenter is 0.5 km/s. Results show that controlling the Lift directions makes possible to increase or reduce the energy variations of the spacecraft.

INTRODUCTION

The Gravity Assist maneuver is designed to give gains or losses of energy for a spacecraft making a fly-by around a target planet. A single Gravity-Assist (GA) with angles of approach of 90° and 270° gives the maximum losses and gains of energy, respectively (Reference 1). The atmospheric influence (Aerogravity-assisted maneuver, as shown in References 2, 3 and 4) is assumed to be made with a ballistic coefficient varying in a large range. The Lift to Drag ratio (L/D) goes up to 9.0 for waveriders spacecraft (Reference 2). Recent developments in hypersonic unmanned vehicles allows the application of these maneuvers for the space exploration, since they are technologically viable. The gravitational influence of the maneuver was studied in detail. Practical applications of the GA are the missions Voyager and Messenger (References 5 to 16).

The impulse applied during the GA allows the reduction or increase of the effect of the combined maneuver, but it is requires the use of fuel. This maneuver have been used in planets and

* Pos-Doctoral researcher, Course of Space Systems, National Institute for Space Research (INPE), Av. Dos Astronautas 1758, São José dos Campos, Brazil, 12227-010, jhonathan.pineros@inpe.br

† General Coordinator of the Graduate School, National Institute for Space Research (INPE), Av. dos Astronautas 1758, São José dos Campos, Brazil, 12227-010, antonio.prado@inpe.br

moons of the solar system (References 17 to 24). In the case of planets with an atmosphere and using a spacecraft with wing-body shape, the GA can be complemented with the aerodynamic forces during the atmospheric flight (References 2 to 4 and 25 to 32). Recently, the combination of the GA with the application of an impulse and passage by the atmosphere was studied. One of the advantages of the application of the Powered Aero-Gravity Assisted Maneuver (PAGAM) is to save propellant and to reduce the cost of the mission, by getting energy from the atmospheric forces (References 33, 34, 35).

The mathematical model used to describe the trajectories around the center of mass of the system is the Restricted Three Body Problem (Reference 36). In this case, the mathematical model is based in our solar system, where the massive body is the Sun, the secondary body is the selected planet and the third body is the massless waverider. Planets of the solar systems like Jupiter, Venus, Mars or the Earth have atmosphere with enough density to generate aerodynamic forces in the spacecraft when it is passing near the pericenter. The influence of the atmosphere during the gravity assist generates the Aero-Gravity Assisted Maneuver (AGAM). With the spacecraft using some type of control in the bank angle during the AGAM, the direction of the aerodynamic forces are controlled to generate orbit changes, increasing or decreasing the effects of the atmosphere. The waveriders spacecraft are ideal to implement the PAGAM because they have maximum Lift-to-Drag ratios, larger than 9.0 in hypersonic flight (Reference 2, 25, 33 to 35). The main goal of this research is to analyze the influence of Powered Aero-Gravity Assisted Maneuvers around Venus and Mars to obtain energy and orbit changes with the variation of the Lift bank angle from -90° to 90° .

MATHEMATICAL MODEL

The system is formed by a set of three bodies: a massive body M_1 (the Sun), a second body M_2 (target planet), both of them moving in Keplerian orbits around their common center of mass, and a third body of infinitesimal mass M_3 (spacecraft), which is orbiting around M_1 when it makes a passage near M_2 (see Figure 1).

The equations of motion are derived from the restricted three-body problem (Reference 36) with the addition of the aerodynamic force AF , that includes the bank angle, changing the vertical component of the Lift and the direction of the Lift component in the plane of the primaries:

$$\ddot{x} = 2\dot{y} + \Omega_x + AFx, \quad (1)$$

$$\ddot{y} = -2\dot{x} + \Omega_y + AFy, \quad (2)$$

$$\ddot{z} = -\frac{(1-\mu)Z}{r_1^3} - \frac{\mu Z}{r_2^3} + AFz, \quad (3)$$

In this case, AFx , AFy and AFz are the aerodynamic force components in the Cartesian rotational system, the potential Ω is a function of the position vectors $r_1 = \sqrt{(x + \mu)^2 + y^2 + z^2}$ and $r_2 = \sqrt{(x - 1 + \mu)^2 + y^2 + z^2}$. The gravitational constant is μ . Equation (4) shows the potential.

$$\Omega = \frac{1}{2}(x^2 + y^2) + \frac{(1-\mu)}{r_1} + \frac{\mu}{r_2}, \quad (4)$$

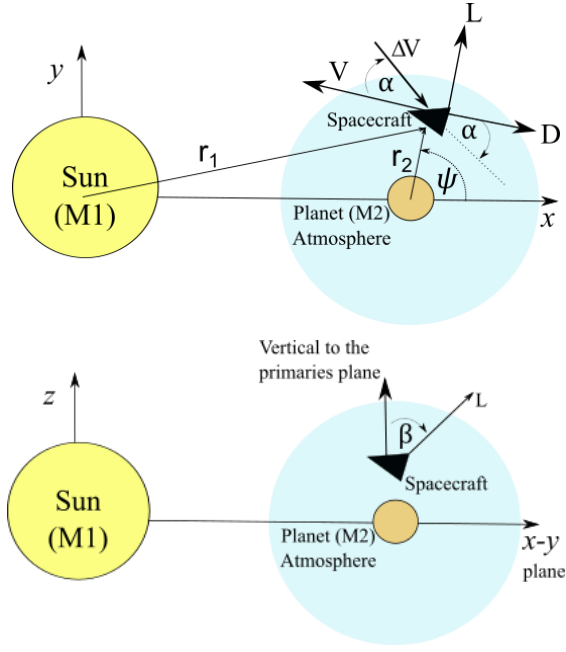


Figure 1. Description of the PAGAM showing the bank angle.

The components of the aerodynamic forces (Lift and Drag in the wind system v_w) are functions of the dynamic pressure $q = \rho v_w^2 / 2$, where ρ is the air density, which is a function of the altitude (Reference 35).

$$AF = L + D, \quad (5)$$

To model of the atmospheric densities are selected to be exponential models, which means that $\rho = \rho_0 e^{(-h/H)}$, where H is the scale height, h the altitude of the spacecraft from the surface of the planet and ρ_0 is the density at this surface. The scale heights selected are 11.1 km for Mars and 15.9 km for Venus. The surface densities are 0.020 kg/m^3 in Mars and 65 kg/m^3 in Venus. Since the Ballistic Coefficient includes the Drag coefficient and the spacecraft area/mass ratio ($C_B = AC_D/2m$), the Drag and Lift forces can be expressed by Equations (6) and (7), (References 33 to 35).

$$D = 2mqC_B, \quad (6)$$

$$L = 2mqC_B(L/D). \quad (7)$$

The Drag force acts opposite to the direction of the motion of the spacecraft and only inside the atmosphere. Due to the fact that the PAGAM is performed to generate energy changes, the Lift is controlled to act orthogonal to the wind velocity vector with components in the positive direction of Z for $-90^\circ < \beta < 90^\circ$. The Lift direction is obtained by controlling the bank angle. In the case of $\beta = 0^\circ$ the Lift is pointing in the vertical direction with respect to the plane X-Y, for $\beta = -90^\circ$ the Lift is acting in the direction of the planet and for $\beta = 90^\circ$ it is in the radial direction. The components of the aerodynamic forces in the wind system are described by equation (8) (Reference 37).

$$AF_{V_w} = \begin{bmatrix} -D \\ L \sin \beta \\ L \cos \beta \end{bmatrix}, \quad (8)$$

The energy variations, inclination changes and semi-major axis are measured in the inertial reference system, before and after the PAGAM. The results are obtained from the numerical integrations of the equations of motion. The total variation of energy ΔE obtained by the maneuver is the difference between the total energy in the inertial reference system, measured before and after the PAGAM (Reference 25,33). Equations (9-11) describe the energy variation. It is assumed that the total variation of energy is due to the kinetic energy variation, because the potential energy is constant, since the maneuver is considered to be instantaneous.

$$E_- = \frac{1}{2}(\dot{X}_I^2 + \dot{Y}_I^2 + \dot{Z}_I^2), \quad (9)$$

$$E_+ = \frac{1}{2}[(\dot{X}_I + \Delta\dot{X}_I)^2 + (\dot{Y}_I + \Delta\dot{Y}_I)^2 + (\dot{Z}_I + \Delta\dot{Z}_I)^2] \quad (10)$$

$$\Delta E = E_+ - E_-. \quad (11)$$

RESULTS

The trajectories analyzed are in the prograde direction, with approach angles of 90° and 270° , and directions for the impulsive maneuver covering angles from -180° to 180° and in the primaries orbital plane (XY). The magnitudes selected for the impulses are 0.0 and 0.5 km/s, the L/D ratios are 0, 1 and 9. The direction of the Lift force is selected to change as a function of the bank angle, which it is assumed to be constant along the trajectory and orthogonal to the wind velocity vector. The Drag coefficients are proportional to the Ballistic Coefficient (C_B), changing from 0 to 5×10^{-7} km²/kg. The altitudes selected for the periapsis are 153 km for Mars and 330 km for Venus, because they showed to generate interesting trajectories in previous publications (References 25, 33 to 35). When the PAGAM is applied with a bank angle of 90° or -90° , the Lift is acting in the orbital plane XY, generating changes in the energy and in the semi-major axis without changes in the inclination. In the case of bank angle with -90° , the Lift is pointing to the center of the planet and, for 90° , it is pointing in the direction opposite to the planet. When the bank angle is 0° , it indicates that the Lift is orthogonal to the orbital plane of the primaries and it generates the highest inclination changes (Reference 35). The canonical units are used, where one canonical unit of distance is equivalent to the mean semi-axis from the orbit of the planet around to the Sun and, for the velocity, it is equivalent to the orbital velocity. For the specific energy is used the square of the orbital velocity, the values are 24.07 km/s for Mars and 35.02 km/s for Venus. More than 100.000 trajectories were simulated and analyzed.

To analyze the results, it was selected the cases with L/D = 9, because they generate the higher influence of the Lift in the trajectories and significant changes in the energy. Trajectories with L/D = 0 does not change as a function of the bank angle, because the Lift force is null for all the trajectories, so the trajectories are only affected by Drag. The Figures 2 to 15 shows the results of trajectories in Mars and Venus. In the case of Venus, for bank angles lower than 0° , highest ballistic coefficients generate aero-capture and orbital decay due to the air density and the proximity of the Sun. In this case, negative bank angles reduce the effective ballistic coefficients for the AGAM.

Three sections of maneuvers are analyzed. The first one for the range $0^\circ < \beta < 90^\circ$, when the Lift has components in the direction opposite to the planet and with a vertical component with respect to the XY plane. The second one is for when $\beta = 0^\circ$ and the third one is for $-90^\circ < \beta < 0^\circ$, when the Lift is in the direction of the planet. In all cases it is observed that the influence of the 0.5 km/s impulse generates more energy changes and dominates the trajectories, compared to the AGAM or maneuvers without impulse. This phenomenon is observed when the red and blue regions (vertical in the cases of AGAM) are horizontal in the figures when the PAGAM is applied (see Figures 2 to 15).

For approach angles of 90° and positive values for the bank angle, the red color represents losses of energy and the blue color the energy gains. All the trajectories show losses of energy, decreasing the losses with the increase of the ballistic coefficient (blue). It means that the Lift and Drag coefficients are maximums, reducing the velocity changes and the duration of the atmospheric flight. The Lift direction is opposite to the planet and the gains in altitude reduce the effects of the density. The reduction of the bank angle reduce the component of Lift in the plane XY and increases the energy losses, which is observed by the changes in the energy from -7.3×10^{-3} CU ($\beta = 90^\circ$) to -7.7×10^{-3} CU ($\beta = 30^\circ$) in the case of Mars and -0.136 CU to -0.146 CU in the case of Venus. The reduction of the bank angle indicates a reduction of the Lift in the plane that contributes to the maneuver. The same behavior is observed in Venus and Mars (see Figures 2, 3, 4, 5, 6, 7 top and left).

When the approach angle is 270° , the energy variations are positive and the lowest energy variations are reached at the maximum ballistic coefficient region (red zone). In this case, the increment of the vertical component of the Lift or the reduction of the bank angle reduce the energy losses, as observed in the increment of the values in the red section from 7.0×10^{-3} CU to 7.4×10^{-3} CU in Mars and 0.128 CU at $\beta=90^\circ$ to 0.138 CU at $\beta=30^\circ$ in Venus. Comparing the maneuvers with the AGAM with approach angle of 90° , the influence of the approach angle of 270° generates positive variations of energy. The inverse behavior is observed with the increase of the ballistic coefficient. The reduction of Lift in the radial direction increases the influence of the gravity assist and reduce the energy losses.

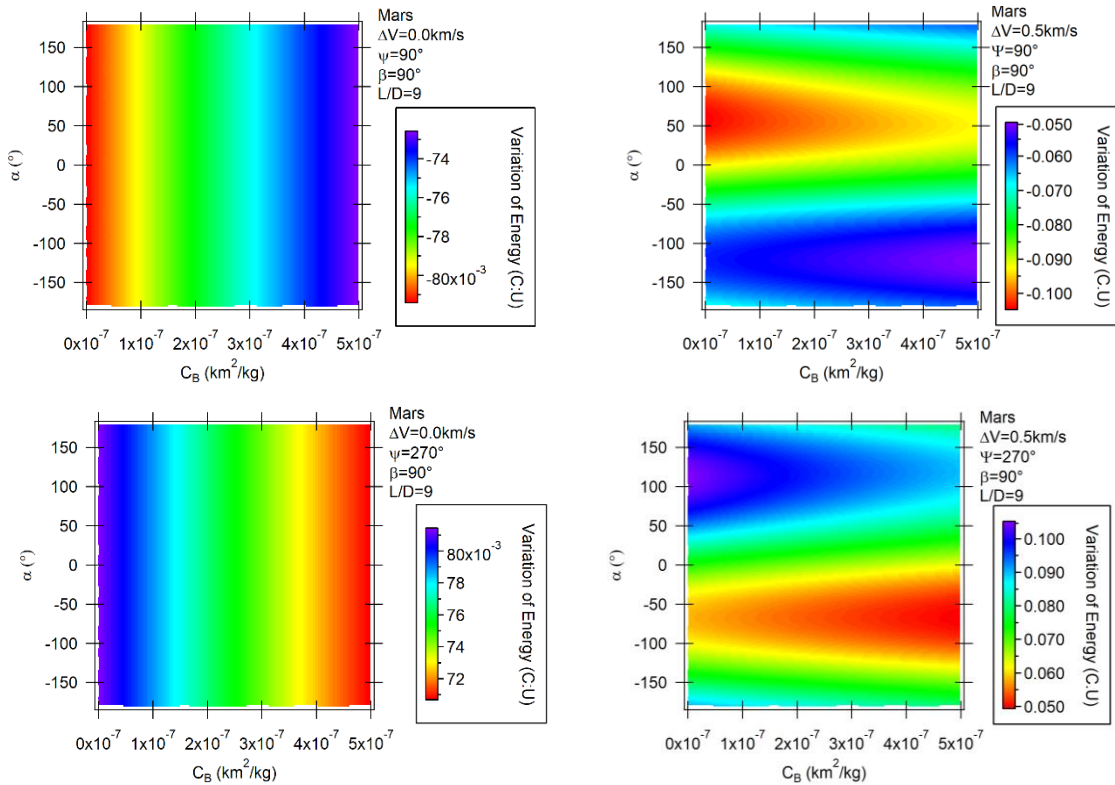


Figure 2. Variations of energy for PAGAM-M with $\beta = 90^\circ$, $L/D = 9$ $\Psi = 90^\circ$ (upper), 270° (lower) and $\Delta V = 0.0$ (left), 0.5 km/s (right).

The application of the impulse generates the PAGAM (right side of the Figures). During this new maneuver, the principal energy variations are presented in regions with attack angles between 0° and 120° , with losses of energy for approach angles of 90° ; -120° to 0° for an approach angle of 270° . In the same way of the AGAM, the region of energy gains and losses are inverted for the approach angles of 90° to 270° in the PAGAM. Initially, for the highest values of the bank angle, the maximum and minimums energy variation zones are distributed in the highest and lowest ballistic coefficients sections. When the bank angle is increased, the reduction of the influence of the Lift force in favor or opposing to the gravity of the planet transform the initial blue and red regions of the energy variations in horizontal lines. In other words, for $\beta = 0^\circ$; the energy losses and gains are functions of the angle of attack and do not show changes as a function of the ballistic coefficient. For approach angles of 90° , the regions of losses of energy are located at the lowest ballistic coefficients with angle of attack around 60° and the direction of the impulse is against the movement of the spacecraft and pointing to the planet. The highest values of C_B indicate that Lift reduces the influence of the impulse in the direction of the planet, reducing the energy losses for angles of -120° . In the trajectories where the approach angle is 270° , the minimum energy variations are presented at the angle of attack of -60° and maximum C_B ; the impulse acts in the Lift direction and against the motion of the spacecraft, reducing the gravitational effect of the maneuver. In both cases, the main contribution of the gravity assisted to the whole maneuver is when C_B is minimum and the impulse is applied between 60° and 120° and acting in the direction of the gravity to increment the curvature angle and the effects of the swing-by.

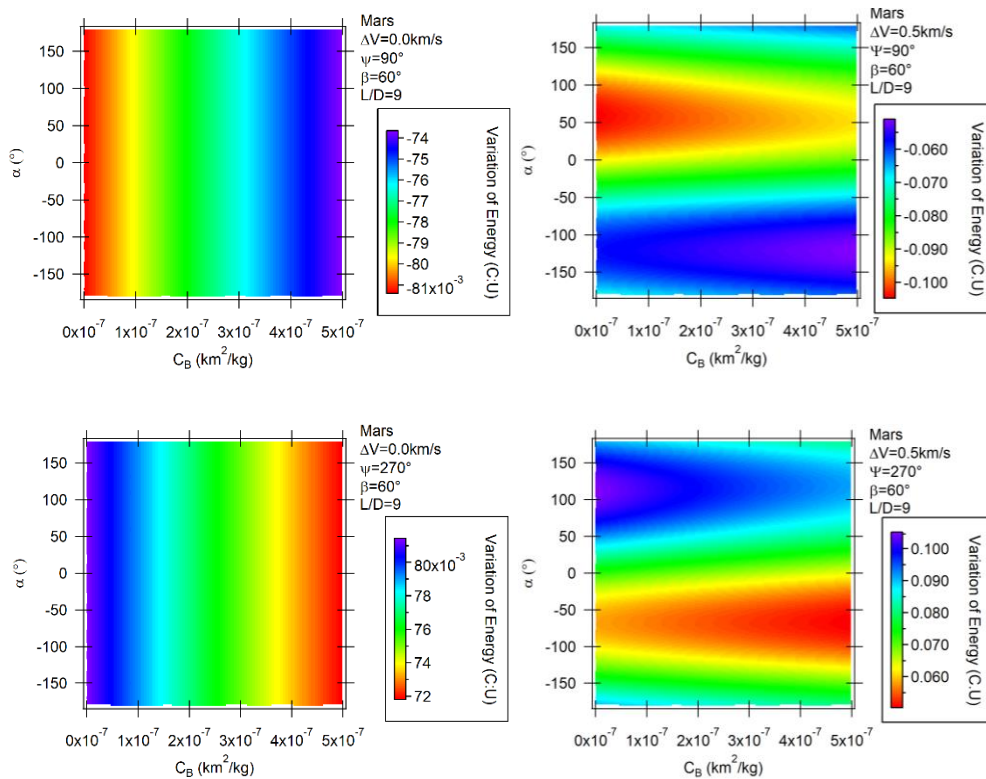


Figure 3. Variations of energy for PAGAM-M with $\beta = 60^\circ$, $L/D = 9$ $\Psi = 90^\circ$ (upper), 270° (lower) and $\Delta V = 0.0$ (left), 0.5 km/s (right).

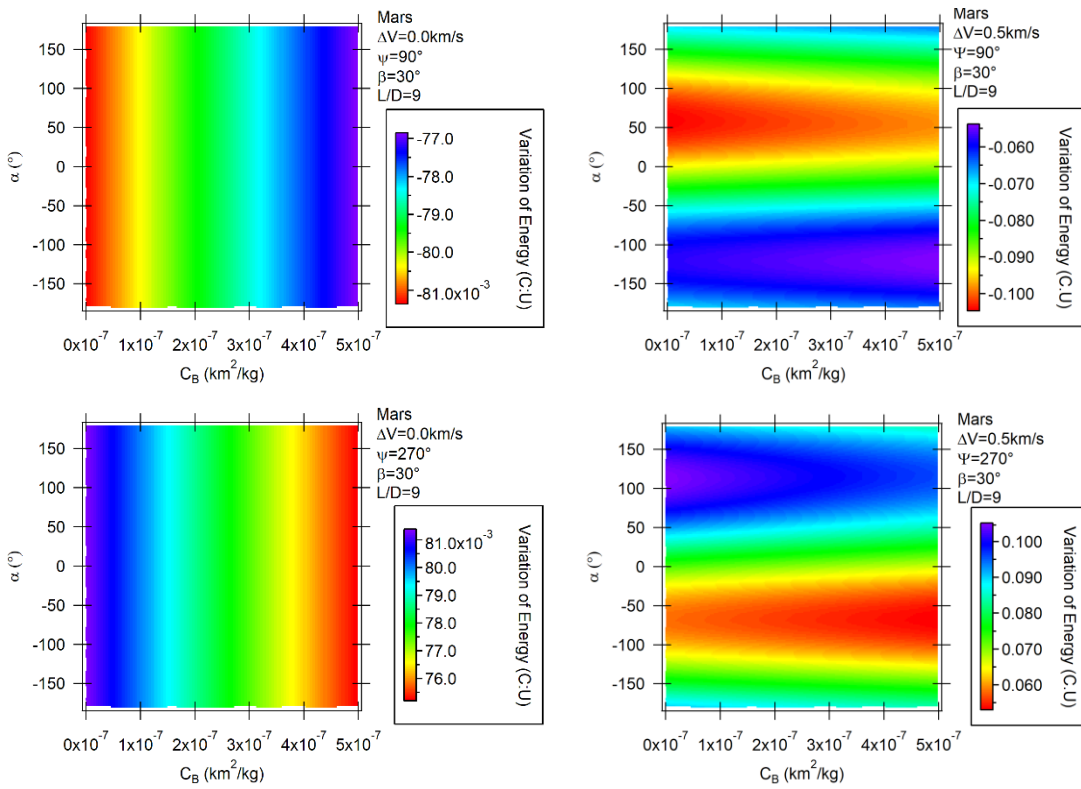
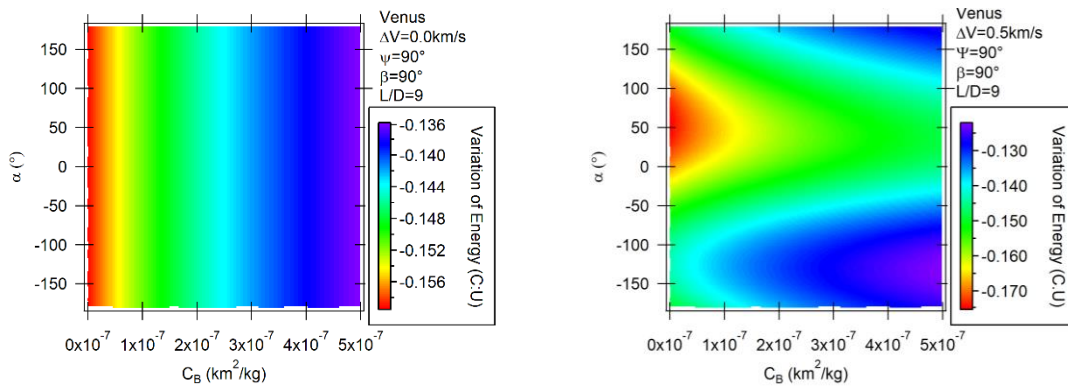


Figure 4. Variations of energy for PAGAM-M with $\beta = 30^\circ$, $L/D = 9$ $\Psi = 90^\circ$ (upper), 270° (lower) and $\Delta V = 0.0$ (left), 0.5 km/s (right).



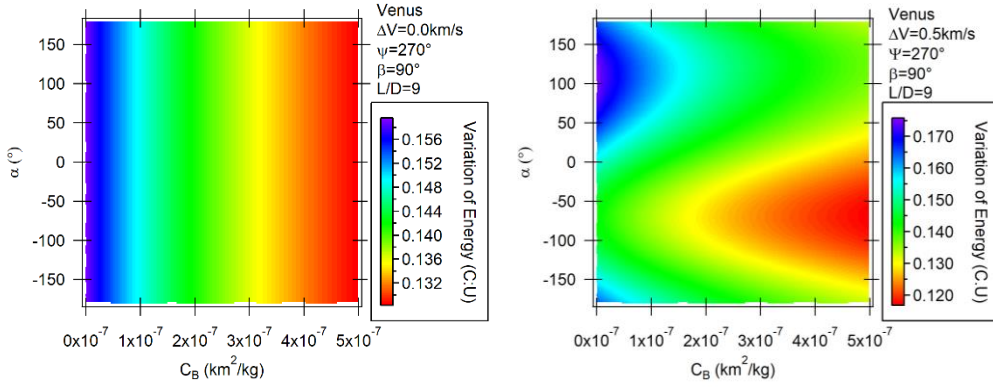


Figure 5. Variations of energy for PAGAM-V with $\beta = 90^\circ$, $L/D = 9$ $\Psi = 90^\circ$ (upper), 270° (lower) and $\Delta V = 0.0$ (left), 0.5 km/s (right).

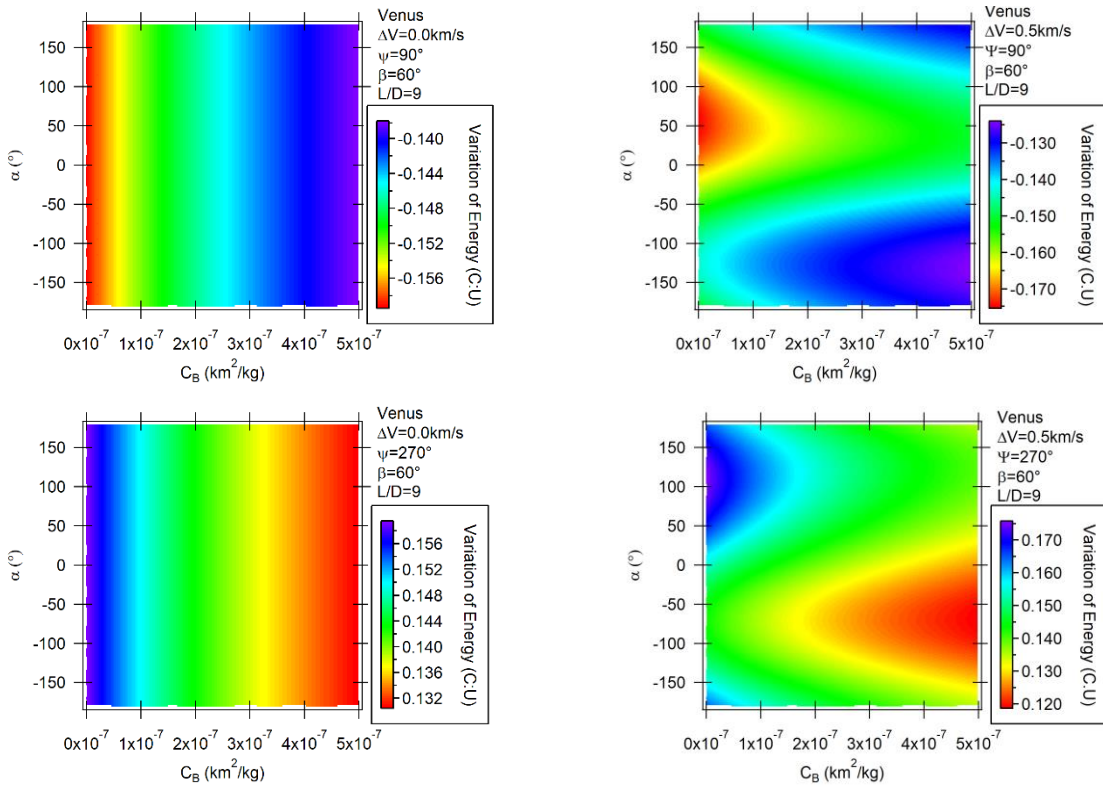


Figure 6. Variations of energy for PAGAM-V with $\beta = 60^\circ$, $L/D = 9$ $\Psi = 90^\circ$ (upper), 270° (lower) and $\Delta V = 0.0$ (left), 0.5 km/s (right).

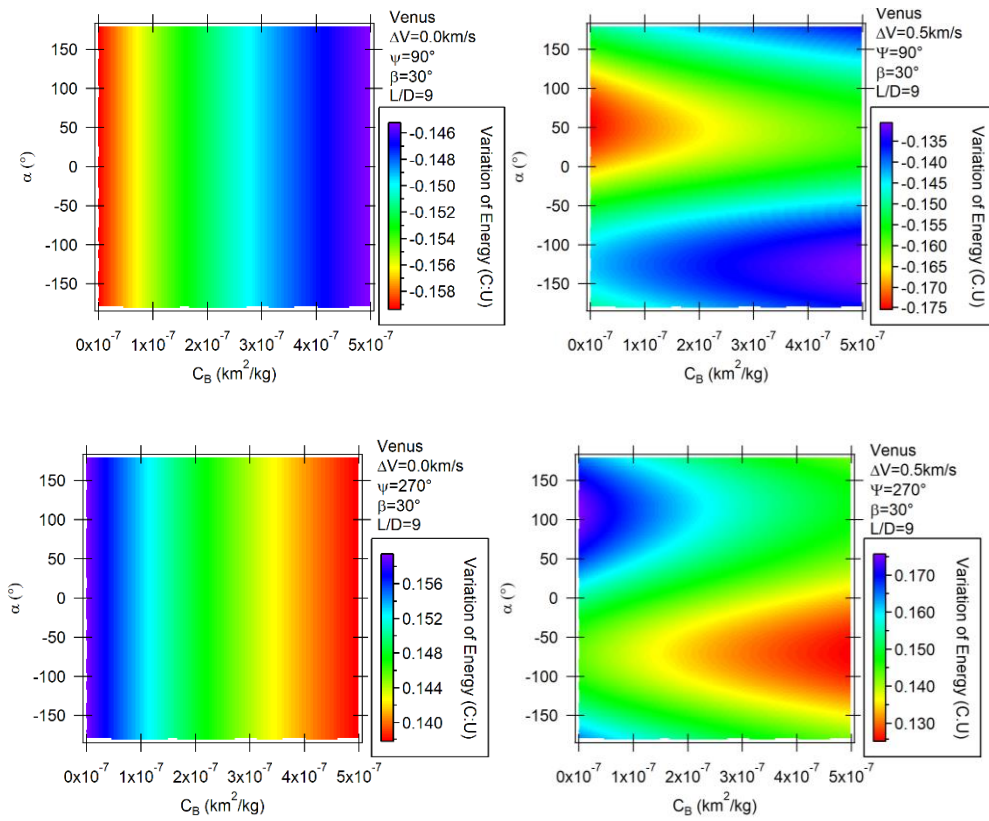
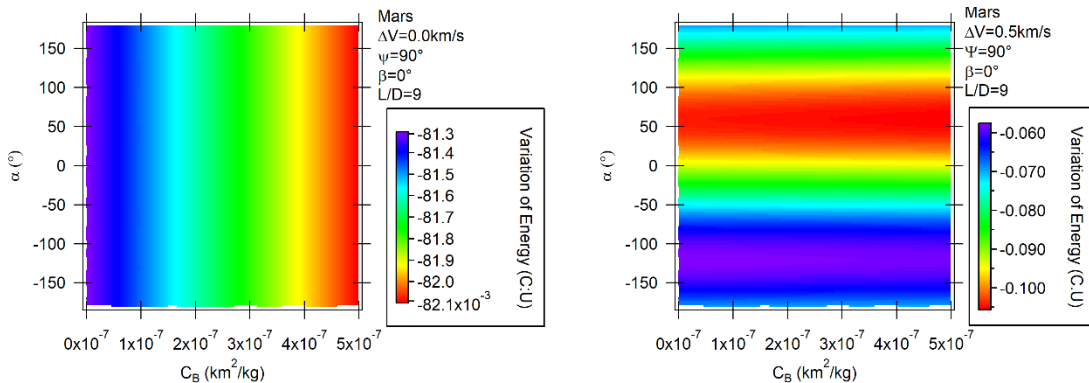


Figure 7. Variations of energy for PAGAM-V with $\beta = 30^\circ$, $L/D = 9$ $\Psi = 90^\circ$ (upper), 270° (lower) and $\Delta V = 0.0$ (left), 0.5 km/s (right).

The AGAM with $\beta = 0^\circ$ shows interesting results. The losses in energy variations are present at $C_B = 0.5 \times 10^{-7} \text{ km}^2/\text{kg}$, and the energy gains are present when the aerodynamic forces are null. The vertical component of the Lift increases the energy losses. For the PAGAM, the regions of losses and gains of energy turn into horizontal lines, indicating a reduction in the effect of the Lift in the energy variations. Energy losses are present at 60° for an approach angle of 90° , and -60° for an approach of 270° and with components against the velocity vector, breaking the spacecraft and reducing the velocity at the end of the maneuver (see Figures 8, 9).



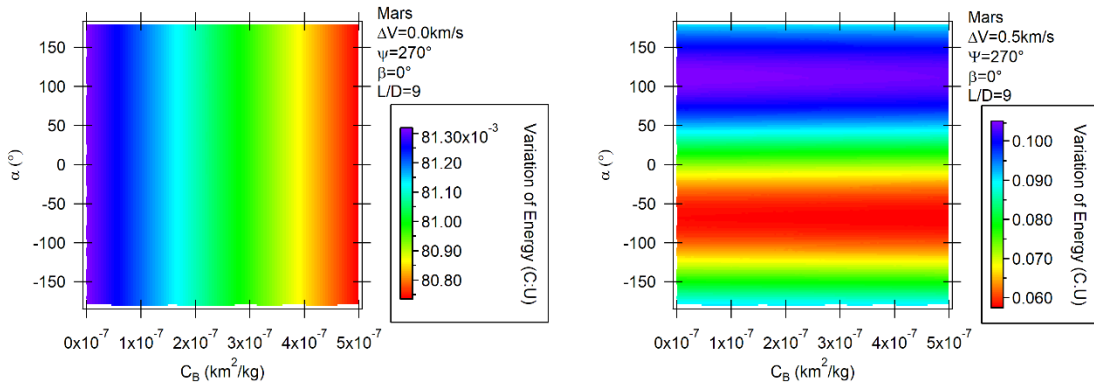


Figure 8. Variations of energy for PAGAM-M with $\beta = 0^\circ$, $L/D = 9$ $\Psi = 90^\circ$ (upper), 270° (lower) and $\Delta V = 0.0$ (left), 0.5 km/s (right).

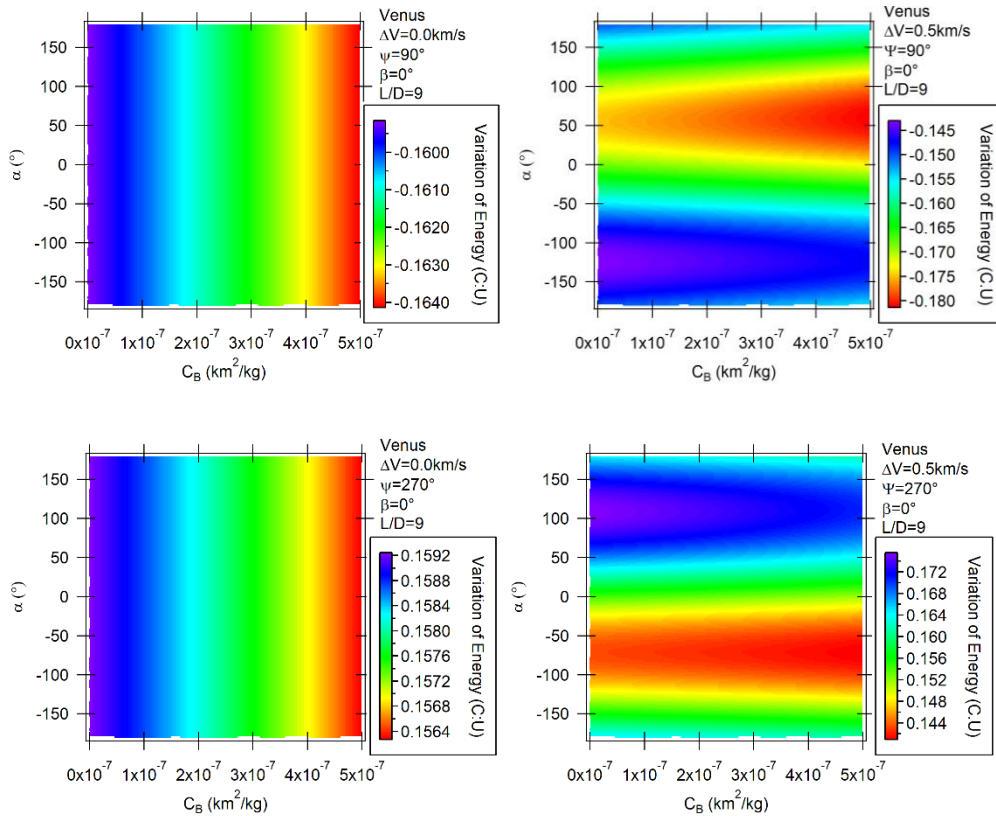


Figure 9. Variations of energy for PAGAM-V with $\beta = 0^\circ$, $L/D = 9$ $\Psi = 90^\circ$ (upper), 270° (lower) and $\Delta V = 0.0$ (left), 0.5 km/s (right).

Trajectories for the bank angle between $-90^\circ < \beta < 0^\circ$ are analyzed only in Mars, because in the case of Venus, the atmospheric density reduce the C_B for the hyperbolic flight. The influence of Lift and the change in the direction affect the energy variations and invert the maximums and minimums positions, compared to the maneuvers with $0^\circ < \beta < 90^\circ$. For an approach angle of 90° , the regions of losses of energy are located at $C_B=0.5 \times 10^{-7}$ km^2/kg and the energy losses increase with

the reduction of the approach angle. For an approach angle of 270° and maximum C_B , the maneuvers increase the energy gains with the reduction of β or with the increment of the Lift component in the plane of the primaries. The Lift in the direction of the gravitational force of the planet increments the effects of the AGAM (see Figures 10, 11, 12, 13, 14, 15).

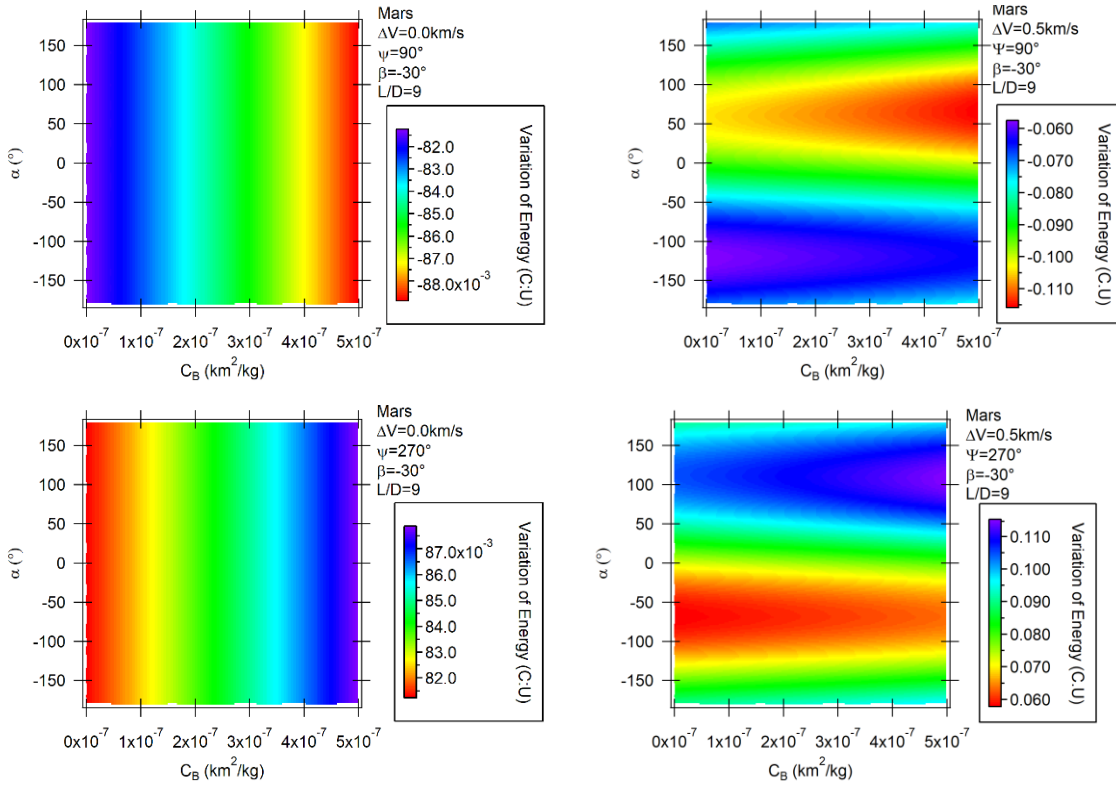
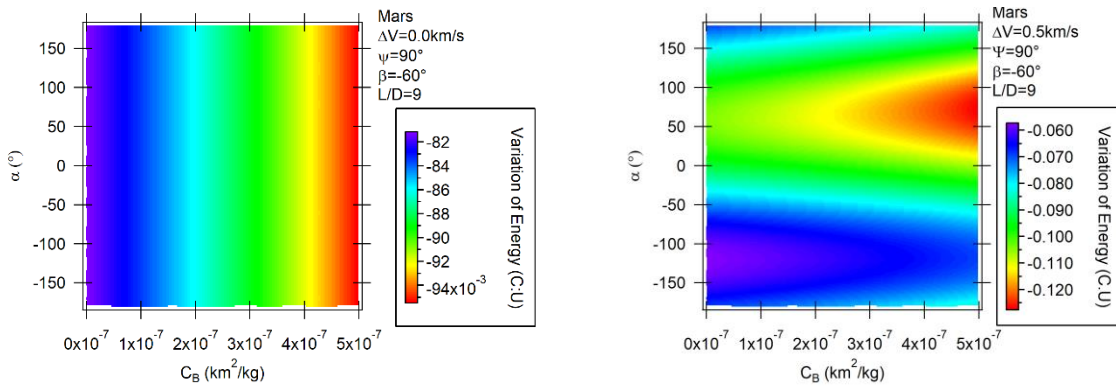


Figure 10. Variations of energy for PAGAM-M with $\beta = -30^\circ$, $L/D = 9$ $\Psi = 90^\circ$ (upper), 270° (lower) and $\Delta V = 0.0$, 0.5 km/s (right).



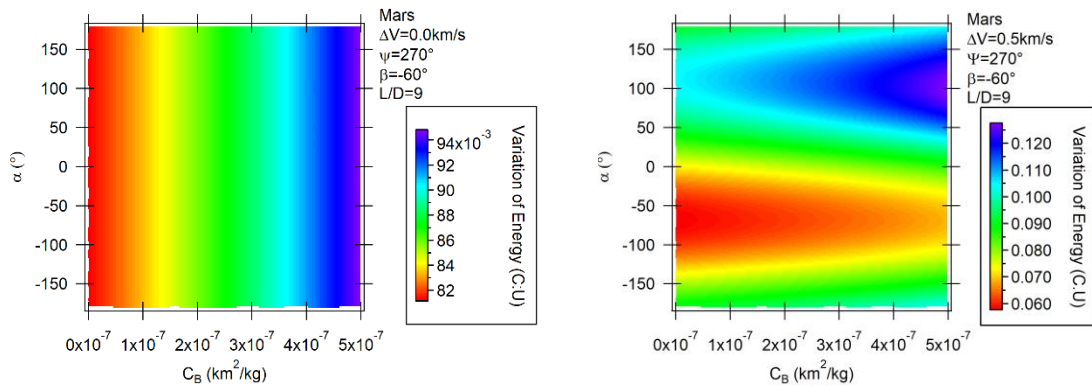


Figure 11. Variations of energy for PAGAM-M with $\beta = -60^\circ$, $L/D = 9$ $\Psi = 90^\circ$ (upper), 270° (lower) and $\Delta V = 0.0$ (left), 0.5 km/s (right).

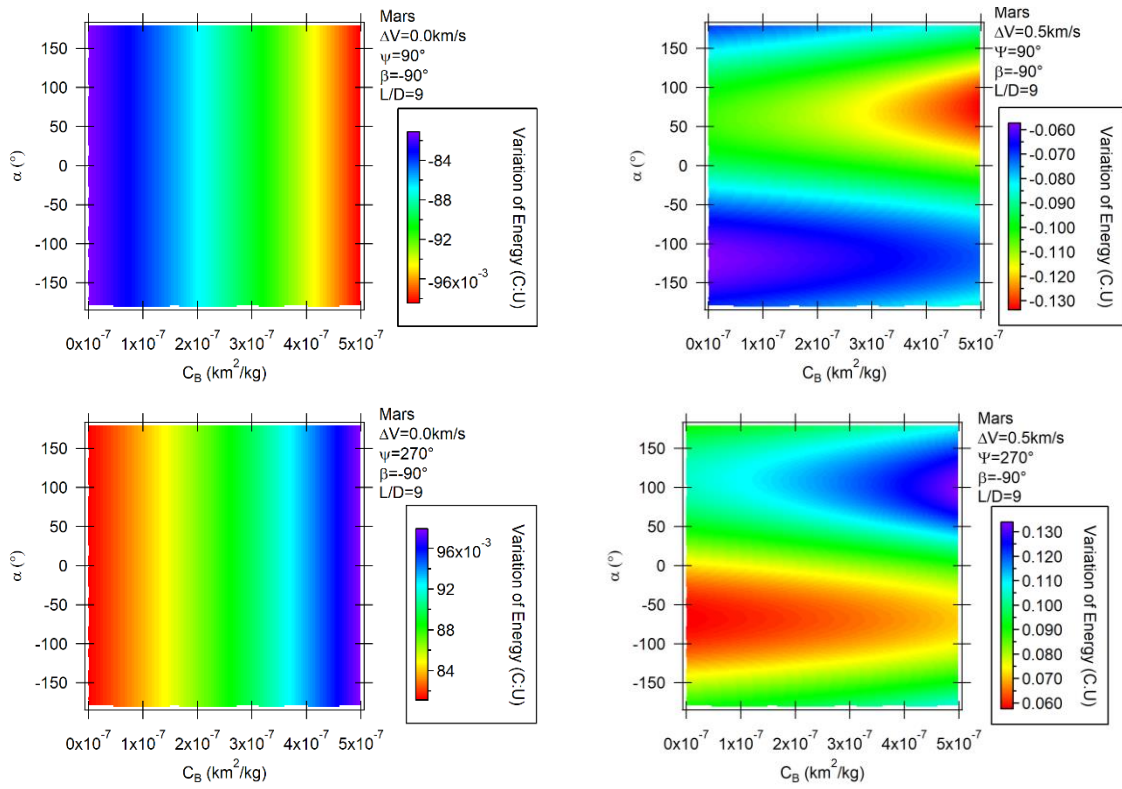


Figure 12. Variations of energy for PAGAM-M with $\beta = -90^\circ$, $L/D = 9$ $\Psi = 90^\circ$ (upper), 270° (lower) and $\Delta V = 0.0$ (left), 0.5 km/s (right).

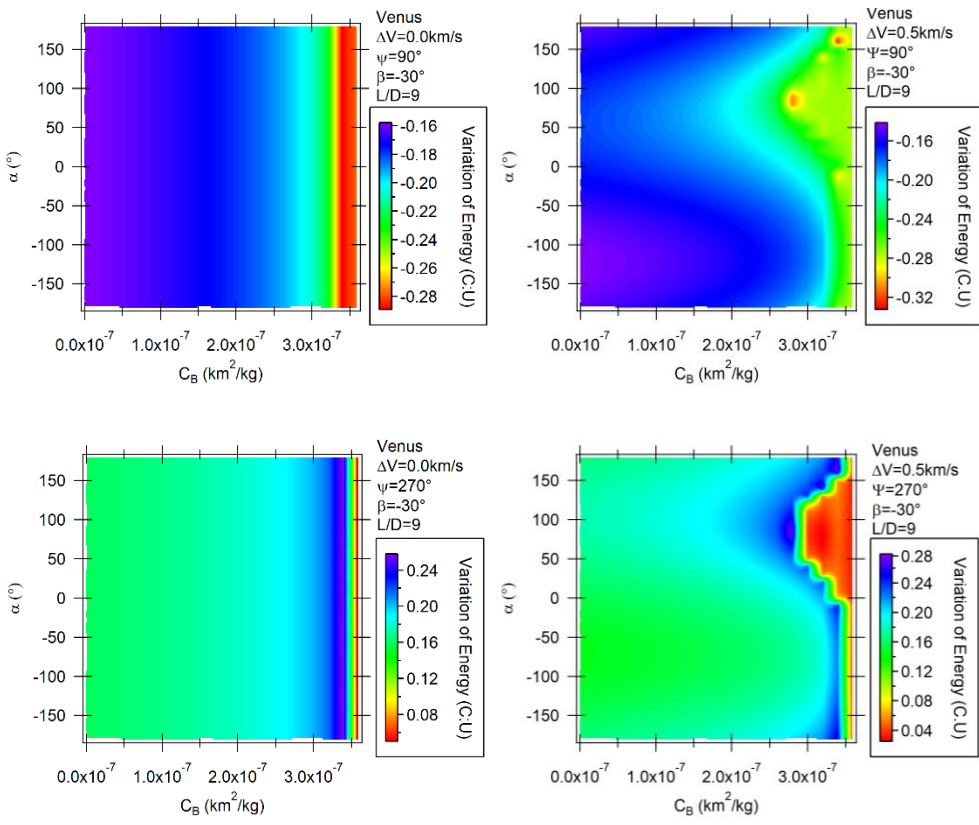
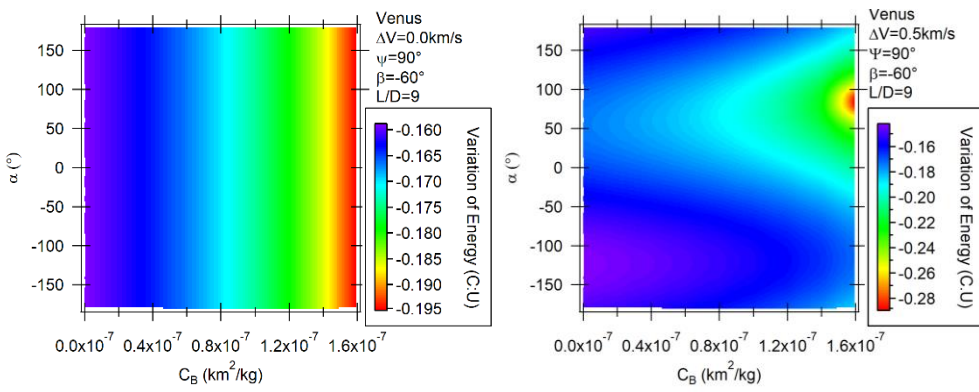


Figure 13. Variations of energy for PAGAM-V with $\beta = -30^\circ$, $L/D = 9$ $\Psi = 90^\circ$ (upper), 270° (lower) and $\Delta V = 0.0$ (left), 0.5 km/s (right).



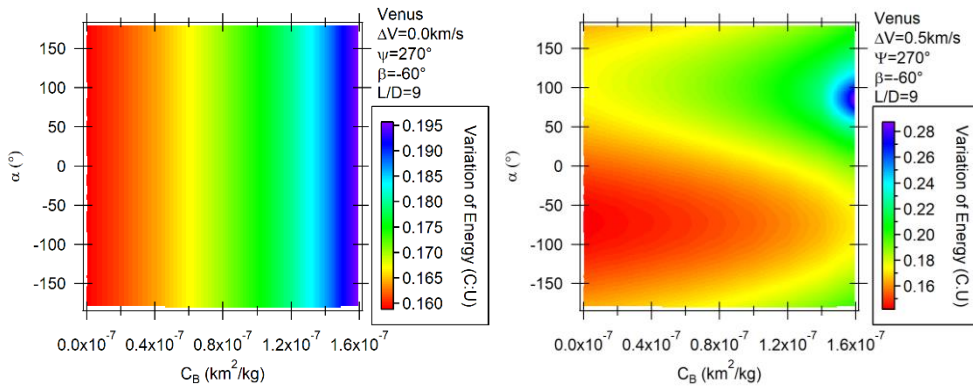


Figure 14. Variations of energy for PAGAM-V with $\beta = -60^\circ$, $L/D = 9$ $\Psi = 90^\circ$ (upper), 270° (lower) and $\Delta V = 0.0$ (left), 0.5 km/s (right).

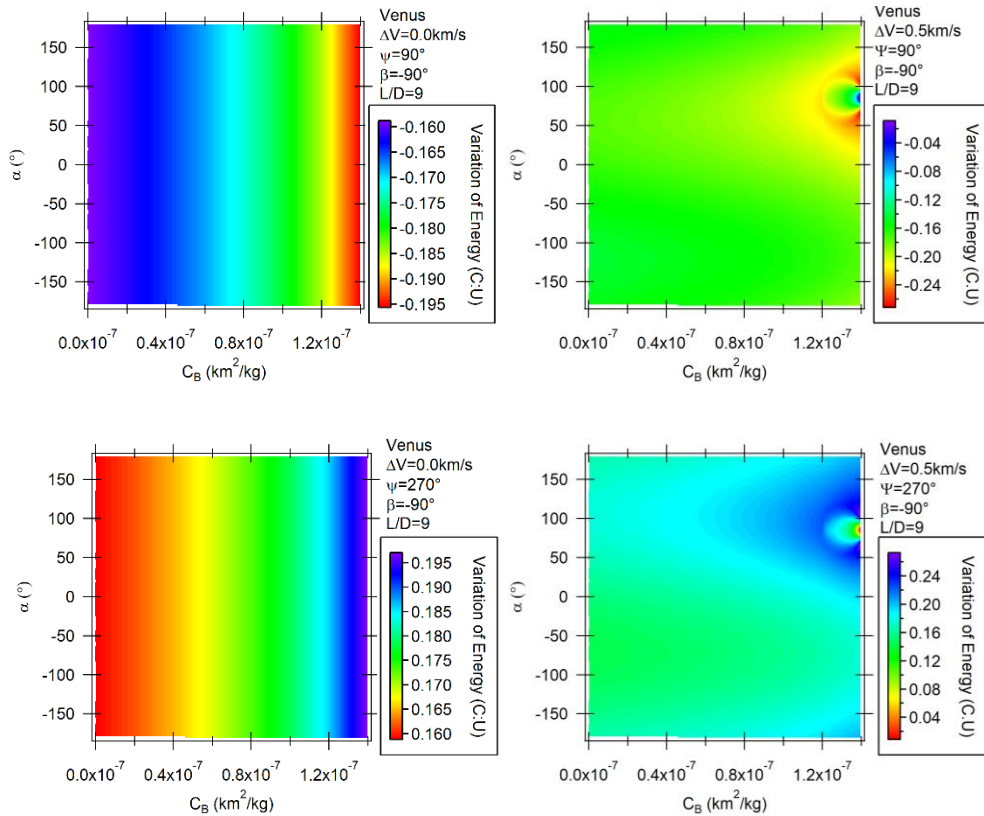


Figure 15. Variations of energy for PAGAM-V with $\beta = -90^\circ$, $L/D = 9$ $\Psi = 90^\circ$ (upper), 270° (lower) and $\Delta V = 0.0$ (left), 0.5 km/s (right).

CONCLUSIONS

The powered aero-gravity-assisted maneuver with the presence of Drag and control in the direction of the Lift force using the bank angle were studied around the planets Venus and Mars, by numerical integrations of the equations of motion. The goal was to determine the changes in the

orbit of the spacecraft due to the direction of the bank angle. More than 100.000 cases were simulated and presented.

The results were divided in three sections, i) for $0^\circ < \beta < 90^\circ$; ii) $\beta = 0^\circ$ and iii) $-90^\circ < \beta < 0^\circ$. In the case of $\beta = 0^\circ$, the Lift is acting in the vertical direction with respect to the plane XY and it reduces its influence during the AGAM and the PAGAM. This is observed due to the location of the minimum energy variations at the maximum ballistic coefficient for the two approach angles, showing a reduction of the energy of the maneuver proportional to the increment of the C_B . In the PAGAM the energy variations are distributed in horizontal sections because the Lift component is orthogonal to the gravitational force, and the energy variations in the PAGAM depends on the direction of the impulse. The PAGAM results for an approach angle of 90° are the opposite, compared to the ones obtained for the angle of approach of 270° .

With the variations of the bank angle, it is possible to observe the influence of the direction of the Lift in the AGA and PAGA maneuvers. Implementing this method, it is possible to control the energy variations along the trajectory for different applications, changing the inclination, increasing the influence of the gravitational and aerodynamic forces and reducing the cost of the mission due to the application of the aerodynamic forces instead of propulsion. The reduction of the bank angle decreases the influence of the Lift in the plane and, in the case of positive bank angles, it reduces the influence of the gravity and drag in the maneuver. For negative values of the bank angle, the Lift increases the influence of the swing-by, because it is in the same direction of the gravitational force of the planet. It also increases the duration of the atmospheric flight. For an angle of approach of 90° , the reduction of β increases the energy losses and, for an approach angle of 270° , it increases the energy gains. Results of PAGAM show regions of maximum and minimum variations that are symmetric when the bank angle is opposite. The variations in the direction of Lift affect the energy variations, changing the maximum and minimum zones according to the bank angle position.

ACKNOWLEDGMENTS

The authors wish to express their appreciation for the support provided by the grants # 406841/2016-0 and 301338/2016-7 from the National Council for Scientific and Technological Development (CNPq); grants #2016/24561-0 and 2016/14665-2, from São Paulo Research Foundation (FAPESP), to the financial support from the National Council for the Improvement of Higher Education (CAPES) and to the National Institute for Space Research (INPE).

REFERENCES

- ¹R. Broucke, The celestial mechanics of gravity assist. *Astrodynamics*, Astrodynamics Conference, AIAA, 1988.
- ²M. Lewis, A. McRonalnd, Design of hypersonic waveriders for aeroassited interplanetary trajectories, *J. Spac. & Rock. AIAA*. 29-5 (1992).
- ³G. Henning, P. Edelman, M. Longuski, Design and optimization of interplanetary aerogravity-assist tours, *J. Spac. & Rock. AIAA*. 51-6 (2014).
- ⁴A. Mazzaracchio, Flight-path guidance for aerogravity-assit maneuvers on hyperbolic trajectories. *Journal of guidance, J. Gui. Cont. & Dyn. AIAA*. 38-2 (2015).
- ⁵D'Amario, L.A., Byrnes, D.V., Stanford, R.H., 1981. A new method for optimizing multiple-flyby trajectories. *Journal of Guidance, Control and Dynamics* 4, 591–596. Doi: 10.2514/3.56115
- ⁶D'Amario, L.A., Byrnes, D.V., Stanford, R.H., 1982. Interplanetary trajectory optimization with application to Galileo. *Journal of Guidance, Control and Dynamics* 5, 465–471. Doi: 10.2514/3.56194
- ⁷J. Deerwester. Jupiter Swingby missions to the Outer Planets. *J. Spac. & Rock..* 3 (10), 1564-1567, 1966.

- ⁸Flandro, G., 1966. Fast reconnaissance missions to the outer solar system utilizing energy derived from the gravitational field of Jupiter. *Acta Astronautica* 12 (4).
- ⁹Grard, R., 2006. Mercury: The Messenger and BepiColombo missions: a concerted approach to the exploration of the planet. *Advances in Space Research*, 38, 563. Doi: 10.1016/j.asr.2006.06.015
- ¹⁰Hollister, W. M., Prussing, J. E. Optimum Transfer to Mars Via Venus. *Astronautical Acta*, 12(2), 169-179, 1966
- ¹¹McNutt Jr., R.L., Solomon, S.C., Grard, R., Novara, M., Mukai, T., 2004. An international program for mercury exploration: synergy of Messenger and Bepicolombo. *Advances in Space Research* 33, 2126–2132. Doi: 10.1016/S0273-1177(03)00439-3
- ¹²McNutt Jr., R.L., Solomon, S.C., Gold, R.E., Leary, J.C., 2006. The messenger mission to mercury: development history and early mission status. *Advances in Space Research* 38, 564–571. Doi: 10.1016/j.asr.2005.05.044
- ¹³Negri, R. B, Prado, A. F. B. A., Sukhanov, A. Studying the errors in the estimation of the variation of energy by the "patched-conics" model in the three-dimensional swing-by. *Celestial Mechanics*. To be published.
- ¹⁴Niehoff, J.C. Gravity-Assisted Trajectories to Solar-System. *Journal of Spacecraft and Rockets*. 3 (9), 1351-1356, 1966.
- ¹⁵Prado, A.F.B.A., 1997. Close-approach trajectories in the elliptic restricted problem. *Journal of Guidance, Control and Dynamics*, 20, 797-802. Doi: 10.2514/2.4115
- ¹⁶Prado, A. F. B. A. A comparison of the "patched-conics approach" and the restricted problem for swing-bys. *Advances in Space Research*, 40, 113-117, 2007.
- ¹⁷Santos, D.P.S., Prado, A.F.B.A., Casalino, L., Colasurdo, G., 2008. Optimal trajectories towards near-earth-objects using Solar electric propulsion (sep) and gravity assisted maneuver. *Journal of Aerospace Engineering, Sciences and Applications* 1(2), 51–64.
- ¹⁸Casalino, L, Colasurdo, G., Pastrone, D.: Simple Strategy for Powered Swing-By. *Journal of Guidance, Control and Dynamics* 22(1), 156-159, 1999a.
- ¹⁹Casalino, L., Colasurdo, G., Pastrone, D.: Optimal Low-Thrust Scape Trajectories Using Gravity Assist. *Journal of Guidance, Control and Dynamics*, 22 (5), 637-642, 1999b.
- ²⁰Ferreira, A.F.S., Prado, A.F.B.A., Winter, O.C., 2015. A numerical study of powered Swing-Bys around the Moon. *Advances in Space Research*, 56, 252-272. Doi:10.1016/j.asr.2015.04.016
- ²¹Ferreira, A. F., Prado, A. F. B. A., Winter, O.C., Santos, D. P. S. Effects of the eccentricity of the primaries in a powered Swing-By maneuver. *Advances in Space Research*, 59 (8), 2071-2087, 2017a. DOI: 10.1016/j.asr.2017.01.033
- ²²Ferreira, A. F., Prado, A. F. B. A., Winter, O.C.: A numerical mapping of energy gains in a powered Swing-By maneuver. *Nonlinear Dynamycs*. 89 (2), 791-818, 2017b. Doi: 10.1007/s11071-017-3485-2. To be published
- ²³Prado, A.F.B.A., 1996. Powered Swing-By. *Advances in Space Research*, 19, 1142-1147. Doi: 10.2514/3.21756
- ²⁴Silva, A.F., Prado, A.F.B.A., Winter, O.C., 2013. Powered Swing-By Maneuvers around the Moon. *Journal of Physics Conference Series*, 465, 012001. Doi: 10.1088/1742-6596/465/1/012001.
- ²⁵Gomes, V. Murcia, J. Prado, A. Golebiewska, J. Atmospheric close approaches with the Earth considering drag and lift forces. *Journal of Computational and Applied Mathmathics* 3- 35 (2015).
- ²⁶Armellini, R., Lavagna, M., Ercoli-Finzi, A. Aero-gravity assist maneuvers: controlled dynamics modeling and optimization. *Periodic, Quasi-Periodic and Chaotic Motions in Celestial Mechanics: Theory and Applications*, 391-405. (2006).
- ²⁷Sims, J. Longuski, J. Patel, M. Aerogravity-assist trajectories to the outer planets and the effect of drag. *Journal of Spacecraft and Rockets*, 37(1), 49-55. (2000).
- ²⁸Lavagna, M., Povoleri, A., Finzi, A. Interplanetary mission design with aero-assisted manoeuvres multi-objective evolutive optimization. *Acta Astronautica*, 57(2), 498-509. (2005).
- ²⁹Rao, A. Scherich, A. Cox, S. Mosher, T. A concept for operationally responsive space mission planning using aeroassisted orbital transfer. In *2008 Responsive Space Conference*. (2008).
- ³⁰Elices, T. Maximum Delta-V in the aerogravity assist maneuver. *Journal of Spacecraft and Rockets*, 32(5), 921-922. (1995).

- ³¹Armellin, R., Lavagna, M., Starkey, R., Lewis, M. Aerogravity-assist maneuvers: coupled trajectory and vehicle shape optimization. *Journal of Spacecraft and Rockets*, 44(5), 1051-1059. (2007).
- ³²Johnson, W. Longuski, J. Design of aerogravity-assist trajectories. *Journal of spacecraft and rockets*, 39(1), 23-30. (2002).
- ³³Piñeros, J. O. M, Prado, A. F. B. A. Powered aero-gravity-assist maneuvers considering lift and drag around the Earth. *Astrophysics and Space Science*. 362 (7), Article 120, 2017.
- ³⁴Murcia, J. O, Prado, A. F. B. A, Gomes, M.: Retrograde and Direct Powered Aero-Gravity-Assist Trajectories around Mars. *Revista Mexicana de Astronomía y Astrofísica*. 54 (1), 2018.
- ³⁵Murcia, J. O, Prado, A. F. B. A, Gomes, M.: Application of impulsive aero-gravity assisted maneuvers in Venus and mars to change the orbital inclination of a spacecraft. *AIAA Astrodynamics Specialist Conference*, (2017).
- ³⁶S. Szebehely, *Theory of orbits the restricted problem of three bodies*, Academic Press, New York, 1967.
- ³⁷Zipfel, P.: *Modeling and Simulation of Aerospace vehicle dynamics*, AIAA, New York, (2007).